



**ASME Accepted Manuscript Repository**

**Institutional Repository Cover Sheet**

Helen Hewitt

*First*

*Last*

ASME Paper Title: A framework for tolerance modeling based on parametric space envelope

Authors: Luo, Chen, Franciosa, Pasquale, Mo, Zhijie and Ceglarek, Darek

ASME Journal Title: Journal of Manufacturing Science and Engineering

Volume/Issue \_\_\_\_\_ 146(6) \_\_\_\_\_ Date of Publication (VOR\* Online)  
\_\_\_\_\_ 17.04.2020 \_\_\_\_\_

ASME Digital Collection URL: <https://asmedigitalcollection.asme.org/manufacturingscience/article-abstract/142/6/061007/1081978/A-Framework-for-Tolerance-Modeling-Based-on?redirectedFrom=fulltext>

DOI: <https://doi.org/10.1115/1.4046743>

\*VOR (version of record)

**Manuscript version: Author's Accepted Manuscript**

The version presented in WRAP is the author's accepted manuscript and may differ from the published version or Version of Record.

**Persistent WRAP URL:**

<http://wrap.warwick.ac.uk/136276>

**How to cite:**

Please refer to published version for the most recent bibliographic citation information. If a published version is known of, the repository item page linked to above, will contain details on accessing it.

**Copyright and reuse:**

The Warwick Research Archive Portal (WRAP) makes this work by researchers of the University of Warwick available open access under the following conditions.

Copyright © and all moral rights to the version of the paper presented here belong to the individual author(s) and/or other copyright owners. To the extent reasonable and practicable the material made available in WRAP has been checked for eligibility before being made available.

Copies of full items can be used for personal research or study, educational, or not-for-profit purposes without prior permission or charge. Provided that the authors, title and full bibliographic details are credited, a hyperlink and/or URL is given for the original metadata page and the content is not changed in any way.

**Publisher's statement:**

Please refer to the repository item page, publisher's statement section, for further information.

For more information, please contact the WRAP Team at: [wrap@warwick.ac.uk](mailto:wrap@warwick.ac.uk).

# A Framework for Tolerance Modeling Based on Parametric Space Envelope

Chen Luo<sup>1</sup>, Pasquale Franciosa<sup>2</sup>, Zhijie Mo<sup>1</sup> and Dariusz Ceglarek<sup>2</sup>

<sup>1</sup> Department of Mechanical Engineering, Southeast University, Nanjing, China; 211189

<sup>2</sup> Digital Lifecycle Management (DLM), WMG, University of Warwick, Coventry, CV47AL, UK

E-mails: [chenluo@seu.edu.cn](mailto:chenluo@seu.edu.cn), [P.Franciosa@warwick.ac.uk](mailto:P.Franciosa@warwick.ac.uk), [ZhijieMo@seu.edu.cn](mailto:ZhijieMo@seu.edu.cn), [D.J.Ceglarek@warwick.ac.uk](mailto:D.J.Ceglarek@warwick.ac.uk)

## Abstract

*GD&T tolerance standards are widely used in industries across the world. A mathematical model to formulate tolerance specifications to enable comprehensive tolerance analysis is highly desirable, but difficult to build. Existing methods have limited success on this with form and profile tolerance modeling as a known challenge. In this paper, we propose a novel tolerance modeling framework and methodology based upon parametric space envelope, a purposely built variation tool constructed from base parametric curve. Under proposal, geometric variation (deviation as well as deformation) is modeled and linked to envelope boundary control points' movement. This indirect tolerance modeling brings various benefits. It is versatile and can handle full set of tolerances specified under GD&T standards including form, profile and runout tolerance. The proposal can deal with complex manufacturing part and is capable of providing modeling accuracy required by many applications. The proposed approach has added advantage of facilitating integration of various computer-aided systems to meet emerging industry demands on tolerancing in a new era of digital manufacturing. The proposed methodology is illustrated and verified with an industrial case example on a two-part assembly.*

**Keywords:** *GD&T, tolerance modeling, tolerance analysis, parametric space envelope*

## 1. Introduction

Tolerance is an essential part of design and manufacturing. In real production environment, manufacturing part cannot be produced to completely conform to design intent [1-6]. Tolerance, permissible limit of variation, has been naturally introduced to address this with an aim to safeguard product functional requirement and to meet parts' interchangeable needs. Modern

*Cite as:* Chen, L., Franciosa, P., Zhijie, M., Ceglarek, D., 2020, “A Unified Framework for Tolerance Modeling and Analysis Based on Parametric Space Envelope”, *ASME Trans., Journal of Manufacturing Science and Engineering*, Vol. 142, No. 6, Article No. 061007, June 2020, DOI: <https://doi.org/10.1115/1.4046743>.

tolerance is based on the concept of “Tolerance Zone (TZ)” [7, 8]. All actual part features falling within the TZ belong to an acceptable variational class.

Today many major industries are becoming more global. To reduce cost, many component parts are currently being sourced from suppliers all over the world resulting in the decentralization of design and manufacturing. The need for accuracy in part design and manufacturing is greater now than ever before. It is imperative that the design intent and functionality of the part be clearly communicated between design engineer and the manufacturing plant at global level. Geometric Dimensioning and Tolerancing (GD&T) has been developed and adopted as a more worldwide standard to specify allowable dimensional and geometric variation on manufacturing part. The GD&T methodology is currently used in automotive, heavy equipment, aviation and several other industries. Two prominent GD&T standards are ASME Y14.5 [9] and ISO 1101 standard [10].

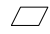



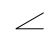



GD&T is a significant improvement over traditional older systems. It is very precise as well as concise relative to the older systems, which rely on extensive non-standard and error-prone notes to make things fully specified. The application of GD&T standards has proven to reduce cost and improve quality, reliability and safety. For example, without GD&T, the tolerance on a hole center is often  $X$  and  $Y$  plus or minus some amount (so-called “square tolerance”). With GD&T, the tolerance is expressed as a round area. The parts, with dimensions fell slightly outside of the square zone but were within a circle that encompassed the square’s corners, are just as functional. As can be seen, GD&T allows for the application of a greater tolerance range, reducing the quantity of functional parts being rejected. Manufacturers thereby increase their first time yield (the ratio of the acceptable assemblies to total assemblies produced) resulting in improved efficiency.

GD&T standards comprise dimensional tolerance and geometric tolerance. Geometric tolerance is further divided into five categories under ASME Y14.5: form, profile, orientation, location and runout. Each of these five categories has sub categories with details shown in Table 1.

It is worth mentioning that the current international standards are created by collecting knowledge from many years of engineering practice. Many tolerances specified did not come out of a mathematical model (nor were attached with such model) but rather out of convention. To implement such tolerance specified by standards, a comprehensive analysis involving all types of dimensional and geometric variations is needed. However, this is only possible if a mathematical model linking tolerance specification to geometric variations exists.

As such, tolerance modeling has drawn wide attention from many researchers. Various methods and models have been developed in the past four decades. This ranges from early one-dimensional (1D) model (i.e., tolerance charts [11, 12]), 2D models [13] to recent 3D models. In three-dimensional space, the position and orientation of a rigid body is defined by three components of translation and three components of rotation. This means that rigid body has six degrees of freedom (DOF). Naturally, many existing 3D tolerance models are built along the idea of DOF. This broadly includes TTRS [14], Deviation Domain [15], Tolerance Map [16] and Jacobian-Torsor model [17]. In general, they are able to provide accurate modeling on ordinary rigid parts (involving translational and rotational displacement). However, a non-rigid,

**Table 1 Dimensional tolerance and geometric tolerance under ASME Y14.5**

TYPE OF TOLERANCE	CHARACTERISTIC	SYMBOL
FORM	STRAIGHTNESS	—
	FLATNESS	
	CIRCULARITY	○
	CYLINDRICITY	
PROFILE	PROFILE OF A LINE	
	PROFILE OF A SURFACE	
ORIENTATION	ANGULARITY	
	PERPENDICULARITY	
	PARALLELISM	//
LOCATION	POSITION	⊕
	CONCENTRICITY	⊙
	SYMMETRY	≡
RUNOUT	CIRCULAR RUNOUT	
	TOTAL RUNOUT	

deformable part involves essentially infinite number of DOF. As such, existing DOF oriented models have inherent difficulty to handle form and profile tolerances. Approximations on form error, attempted by many existing methods, are inaccurate and incomplete in many cases.

Furthermore, existing tolerance modeling methods are not sufficient to cope with new emerging trends in industry, such as Industry 4.0 [18-20] and Digital Twin (DT) [21]. Industry 4.0 shows the current trend of automation and data exchange in manufacturing technologies. DT aims to develop a seamless integration between digital and real world. Core part of that involves the capability to exploit simulation tools throughout the lifecycle of new product and processes.

In view of that, this paper proposes a novel modeling for GD&T standards under parametric space envelope framework. It provides vital link between allowed geometric variation and tolerance specification. Variation (to be modeled) can include deviation (from rigid part) as well as deformation experienced by non-rigid, compliant part. The developed method is versatile to enable modeling all classes of dimensional and geometric tolerances specified by standards including form and profile tolerance. The proposal helps formalize tolerance specifications and enables full three-dimensional tolerance analysis. The fact, that the variation tool under proposed modeling framework is constructed from parametric curves, makes proposed method closely linked to computer-aided design (CAD) techniques. This CAD-driven approach is portable across multiple stages of the product development, from concept to prototyping, to manufacturing and inspection. As such, the developed method can be deployed and integrated with existing CAD and Product Lifecycle Management (PLM) systems to facilitate continuous quality improvement.

This paper is organized as follows. Section 2 provides related work on tolerance modeling. Section 3 presents detailed methodology on tolerance modeling based upon parametric space envelope. Section 4 presents a case example on a two-part assembly using proposed method. Discussions on the proposed modeling framework are provided in Section 5, and Section 6 concludes the analysis.

## **2. Related Work**

In the past four decades, tremendous efforts have been devoted to geometric tolerance modeling for manufacturing and assembly [18]. Researchers are trying to address the challenge

to build a mathematical model of geometric variations that is consistent with tolerance standards and capable of supporting comprehensive tolerance analysis. Many different methods have been proposed.

The offset zone model proposed by Requicha [7, 23] is one of the earliest mathematical methods to construct tolerance zones. Under this method, a tolerance zone is modeled as Boolean subtraction of maximal and minimal object volumes that are obtained by amounts equal to the tolerances on either side. Offset model conforms to tolerance standards. However, it can be applied to rather simple parts as involved computation time for construction and evaluation is considerably high.

Deviation Domain is a three-dimensional (3D) model which relies extensively on degree of freedom concept. Each tolerance zone allows a small amount of variations of target feature within the tolerance zone. These small amounts of variations are represented as small displacement torses (SDT). A torses basically represents three translations and three rotations of a feature with respect to a co-ordinate system. In order to represent the variations of a feature within its tolerance zone, a deviation space is created using the non-invariant components of the SDT. Based on the condition of tolerance feature lying within tolerance zone, inequalities representing the bounds of the tolerance zone are created. These inequalities are then used to create a bounded deviation domain. More details about deviation domain can be found in [15, 24]. Deviation Domain conforms to tolerance standards. However, it can only model certain sets of tolerance specified under GD&T while still having difficulty to model profile tolerance.

To overcome limitations and difficulties of point based SDT approach [25], researchers [17, 26-31] subsequently proposed Jacobian-Torses model. It is essentially the unification of two existing models: the Jacobian's matrix model and the tolerance zone representation model. Jacobian's matrix method is based on the infinitesimal modeling of open kinematic chains in robotics, while tolerance zone representation model uses small displacement screws and constraints to establish the extreme limits between which points and surfaces can vary. These approaches also apply interval algebra as a useful method to take tolerance boundaries into account in tolerance analysis. Jacobian-Torses model is suitable for tolerance modeling related to rigid part but not ideal for non-rigid compliant part.

A Tolerance-Map [16] is a hypothetical Euclidean point-space, the size and shape of which reflects all variational possibilities for a target feature. It is the range of points resulting from a

one-to-one mapping based on the variational possibilities of a feature (within its tolerance-zone) to the Euclidean point-space. These variations are determined by related tolerances that are specified on the feature. The T-Map for any combination of tolerances on a feature is constructed from a basis-simplex and described with areal coordinates. If the mapping is done for  $n$ -types of variation of a feature, a T-Map will be created in  $n$ -dimensional. The basis-simplex will also be of  $n$ -dimensions. For three-dimensional variations of a feature, the corresponding T-Map is normally constructed from four basis points that define its basis-tetrahedron. The shape of the basis-tetrahedron is typically chosen to simplify interpretation of T-map, particularly to decouple rotational and translational displacements in the tolerance zone [32]. T-Map model [16, 33] has the advantage of conforming to the GD&T standards. The downside of the model is that visualization of high dimensional maps is difficult, and the Minkowski operations involved in this model is known to be computationally expensive and not straightforward [34].

Applying the concept of constraints and rigid body motions in kinematics, Desrochers and Clement [31] used six Technologically and Topologically Related Surfaces (TTRS) for dimensioning and tolerancing. According to TTRS, three dimensional surface or features are classified according to their respective degree of invariance under the action of rigid motions. In total, seven main features equivalent to kinematic lower pairs are identified. Each main feature is then described by a unique minimum geometrical reference element (MGRE) that allows combination of elementary geometrical objects. With its extensions [36-39], TTRS has evolved into a general framework which addresses the problem of translating tolerance zones into mathematical key parameters. However, TTRS still has difficulty to handle profile tolerance among other drawbacks [32].

The aforementioned methods and models are broadly built surrounding the concept of degree of freedom (DOF). More details can be found in survey papers [40-45]. None of these models are complete as yet in representing all geometric tolerances specified in the GD&T standards. In particular, they have difficulty to model shape errors to handle profile and symmetry tolerances. In addition, their modeling of tolerance interactions is incomplete (TTRS and Deviation Domain) [32], which will directly impact their modeling accuracy. Furthermore, there are larger issues for existing methods to integrate tolerances across product life cycle (design, manufacturing and inspection) [32].



Data integration across product lifecycle phases and across all computer-aided systems is key part of digital manufacturing. For example, Digital Twin [21, 47-48] refers to a comprehensive physical and functional description of a component, product or system, which includes more or less all information which could be useful in all lifecycle phases. This latest industry development raises new requirements on tolerance modeling. To address the shortcomings of existing methods and take on emerging challenges of the industry, this paper proposes a novel methodology based upon parametric space envelope, a variation tool that is purposely built to aid tolerance modeling.

### 3. Methodology

The modeling framework developed in this paper is based upon parametric space envelope, which is a lattice of grid of control points and constructed from a base parametric curve (such as Bezier curves, B-splines, or NURBS among others). The method applies Free-form Deformation (FFD) technique [49], which is widely used in computer graphics. To illustrate the proposed method, here we use Bezier curve as a base curve to construct the tool. In this way, the created parametric space envelope is trivariate Bezier volume. It is an extension of one dimensional Bezier curve to three dimensional. Its axes are defined by the orthogonal vectors  $s$ ,  $u$  and  $w$ . When target object is enclosed into the variation tool (or Bezier volume), a local parameter coordinate for the target object is then assigned. Whenever boundary control points moved place, the enclosed object gets displaced accordingly. The position of an arbitrary point of the enclosed object is given by [49]:

$$\mathbf{Q}(s, u, w) = \sum_{i=0}^l \sum_{j=0}^m \sum_{k=0}^n B_i^l(s) B_j^m(u) B_k^n(w) \cdot \mathbf{p}_{ijk} \quad (1)$$

where  $\mathbf{Q}$  contains the coordinates of point sampled from the object.  $B_i^l(s)$ ,  $B_j^m(u)$  and  $B_k^n(w)$  are Bernstein polynomial of degree  $l$ ,  $n$  and  $m$ , respectively and defined by  $B_i^l(s) = \binom{l}{i} s^i (1-s)^{l-i}$ .  $\mathbf{p}_{ijk}$  is the  $i, j, k$ -th control point.

GD&T standards comprise dimensional tolerance and geometric tolerance. Geometric tolerance is further divided into five categories (Table 1). Here for ease of presenting our

method, we loosely group geometric tolerances into two: rigid body related tolerances (including orientation and location tolerances) with a focus on deviation modeling; and shape related tolerances (including form, runout and profile tolerances) which involve deformation modeling. Tolerances specified by GD&T are based on the concept of tolerance zone. Tolerance modeling involves building mathematical relationship between geometric variation and related tolerance zone.

**3.1 Dimensional tolerance modeling.** Dimension (length, width, height, diameter, etc.) is the numerical value that defines the size or geometric characteristic of a feature. ASME Y14.5M defines dimensional tolerance as “the total amount a specific dimension is permitted to vary. The tolerance is the difference between the maximum and minimum limits”. Compared with geometric tolerance, dimensional tolerance is straightforward and can be modeled by the proposed method.

If target feature is enclosed into a constructed parametric space envelope, feature’s dimension will deviate from design intent when control points moved along the dimension direction  $\mathbf{v}_{ijk}$  (Fig. 1). In general, the direction of  $\mathbf{v}_{ijk}$  points to increasing dimensional size. Scaling parametric space envelope through control points, the dimension of enclosed feature will increase or decrease accordingly. The deviated feature can be calculated as follows:

$$\mathbf{Q}'(s, u, w) = \sum_{i=0}^l \sum_{j=0}^m \sum_{k=0}^n B_i^l(s) B_j^m(u) B_k^n(w) (\mathbf{p}_{ijk} + t_{ijk} \mathbf{v}_{ijk}) \quad (2)$$

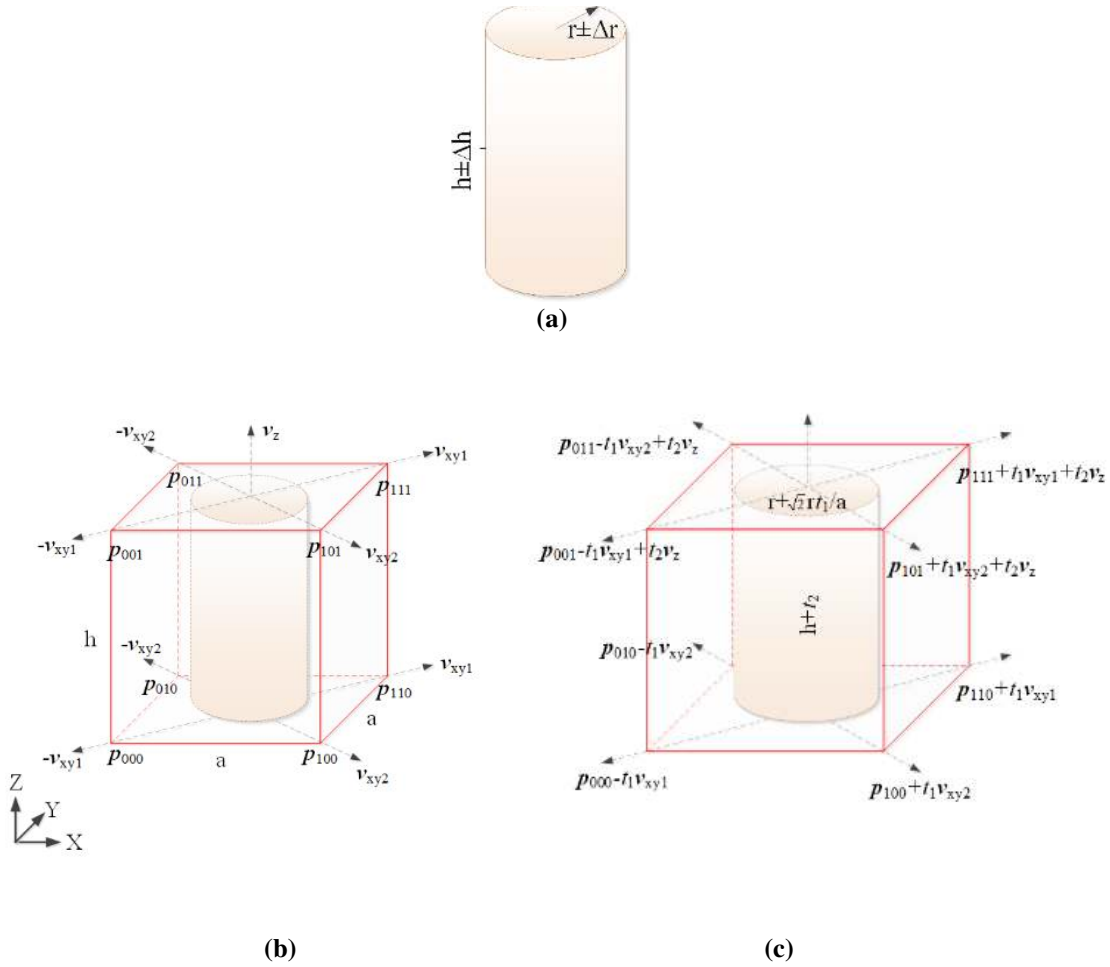
where  $t_{ijk}$  is control points’ moving distance in direction  $\mathbf{v}_{ijk}$  (which is unit vector). And feature’s dimensional deviation is:

$$\Delta \mathbf{Q}(s, u, w) = \sum_{i=0}^l \sum_{j=0}^m \sum_{k=0}^n B_i^l(s) B_j^m(u) B_k^n(w) (t_{ijk} \mathbf{v}_{ijk}) \quad (3)$$

More generally, a feature’s dimensional tolerance is specified as *tol* under GD&T. This tolerance zone can be modeled using Eq. (3). In Fig. 1(a), a cylindrical part with radius  $r$  and height  $h$  is shown. The corresponding dimensional tolerance zone is  $[r-\Delta r, r+\Delta r]$  and  $[h-\Delta h, h+\Delta h]$ , respectively. Applying proposed method, a parametric space envelope (of size  $a \times a \times h$ ) was constructed and imposed on the cylindrical part, where the part is located centrally and coaxes with the variation tool (Fig. 1(b)). If eight corner control points moved simultaneously

outwards along  $\mathbf{v}_{ijk}$  direction by  $t_1$  in Fig. 1(b), then cylinder's radius will increase by  $\frac{\sqrt{2}rt_1}{a}$

(here  $t_1 > 0$  indicates increasing radius while  $t_1 < 0$  indicates decreasing radius). Here  $\mathbf{v}_{111} = \mathbf{v}_{110} = \mathbf{v}_{xy1}$ ,  $\mathbf{v}_{101} = \mathbf{v}_{100} = \mathbf{v}_{xy2}$ ,  $\mathbf{v}_{001} = \mathbf{v}_{000} = -\mathbf{v}_{xy1}$  and  $\mathbf{v}_{011} = \mathbf{v}_{010} = -\mathbf{v}_{xy2}$ . If the top four control points moved vertically upwards along Z axis by  $t_2$ , then cylinder's height will increase by  $t_2$ . As such, dimensional tolerance zone of the diameter and height can be modeled as  $[-\frac{\sqrt{2}rt_1}{a}, +\frac{\sqrt{2}rt_1}{a}]$  and  $[-t_2, +t_2]$ , respectively under the constructed variation tool.



**Fig. 1** Dimensional tolerance modeling based on parametric space envelope

More importantly, the cylindrical part's diameter and height variation can be stacked up and modeled in combination under variation tool in Fig. 1(c). It avoids modeling the two dimensional variation separately and then taking into account the interaction between them in

extra steps. This brings efficiency. In essence, GD&T dimensional tolerance zone can be modeled by scaling the outer parametric space envelope under proposed method.

**3.2 Rigid body related tolerance modeling.** Under GD&T standards, rigid manufacturing parts are typically assigned with tolerances of location and orientation to control translational and rotational displacement. Tolerances of location are subdivided into position, concentricity and symmetry tolerance. Tolerances of orientation include sub-categories of angularity, perpendicularity and parallelism. Here we loosely group them into rigid body related tolerance for ease of presenting the model.

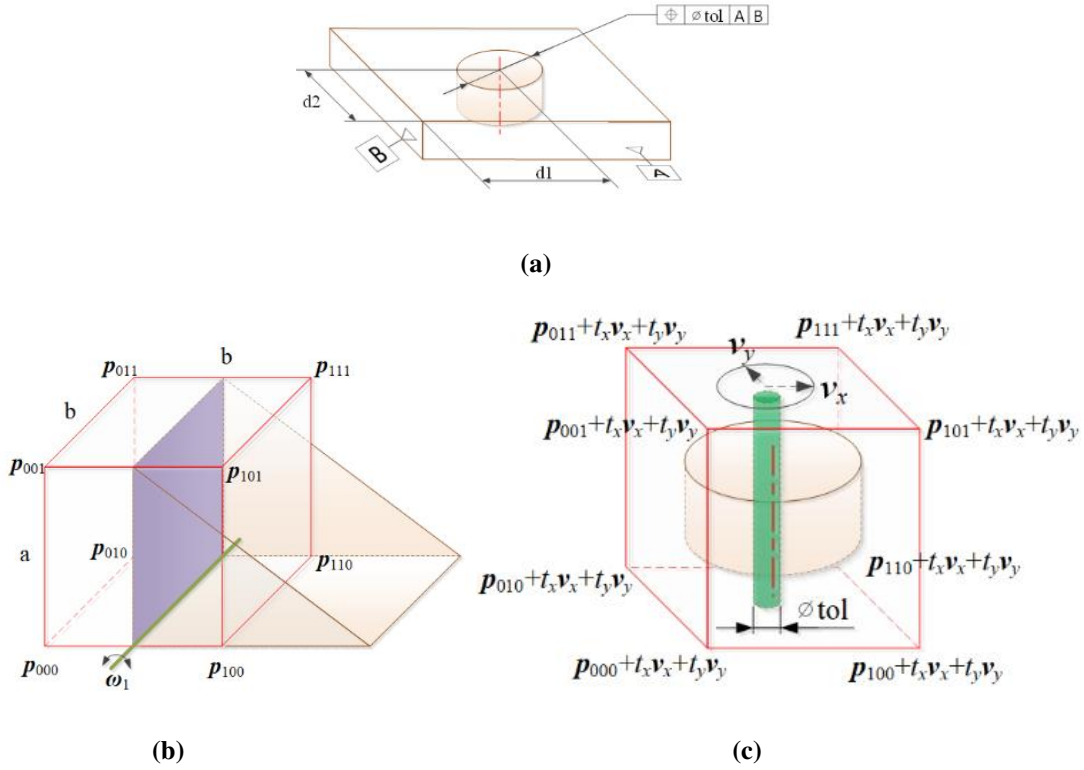
*3.2.1 Translational displacement related tolerance modeling.* Under our proposed modeling framework, enclosed manufacturing part will experience translational deviation when control points moved position in certain direction simultaneously (i.e. maintaining the angle and distance among control points). The displaced feature (or part) can be calculated as follows:

$$\mathbf{Q}'(s, u, w) = \sum_{i=0}^l \sum_{j=0}^m \sum_{k=0}^n B_i^l(s) B_j^m(u) B_k^n(w) (\mathbf{p}_{ijk} + t\mathbf{v}) \quad (4)$$

where  $\mathbf{v}$  is the translation direction and  $t$  is the translational distance of control points. And the translational deviation of the target part is

$$\Delta\mathbf{Q}(s, u, w) = \sum_{i=0}^l \sum_{j=0}^m \sum_{k=0}^n B_i^l(s) B_j^m(u) B_k^n(w) (t\mathbf{v}) \quad (5)$$

If specified location tolerance for a rigid part is  $tol$ , then this tolerance zone can be modeled using Eq. (5). In Fig. 2(a), the position tolerance of the hole in the rigid part was  $tol$ . The position tolerance is in reference to datum planes A and B. If all control points moved position on  $xy$  plane, the displaced feature can be calculated according to Eq. (5). Permitted control point movement satisfies  $\sqrt{t_x^2 + t_y^2} \leq tol$  in this example under constructed parametric space envelope in Fig. 2(c), where  $t_x$  and  $t_y$  are control point displacement in X and Y direction, respectively.



**Fig. 2** Position tolerance modeling based on parametric space envelope

**3.2.2 Rotational displacement related tolerance modeling.** Tolerances of perpendicularity, angularity and parallelism aim to limit angular displacement of a manufacturing part. This can be modeled by the proposed method. If all control points rotate in one direction, enclosed manufacturing part will experience angular displacement and the displaced part is:

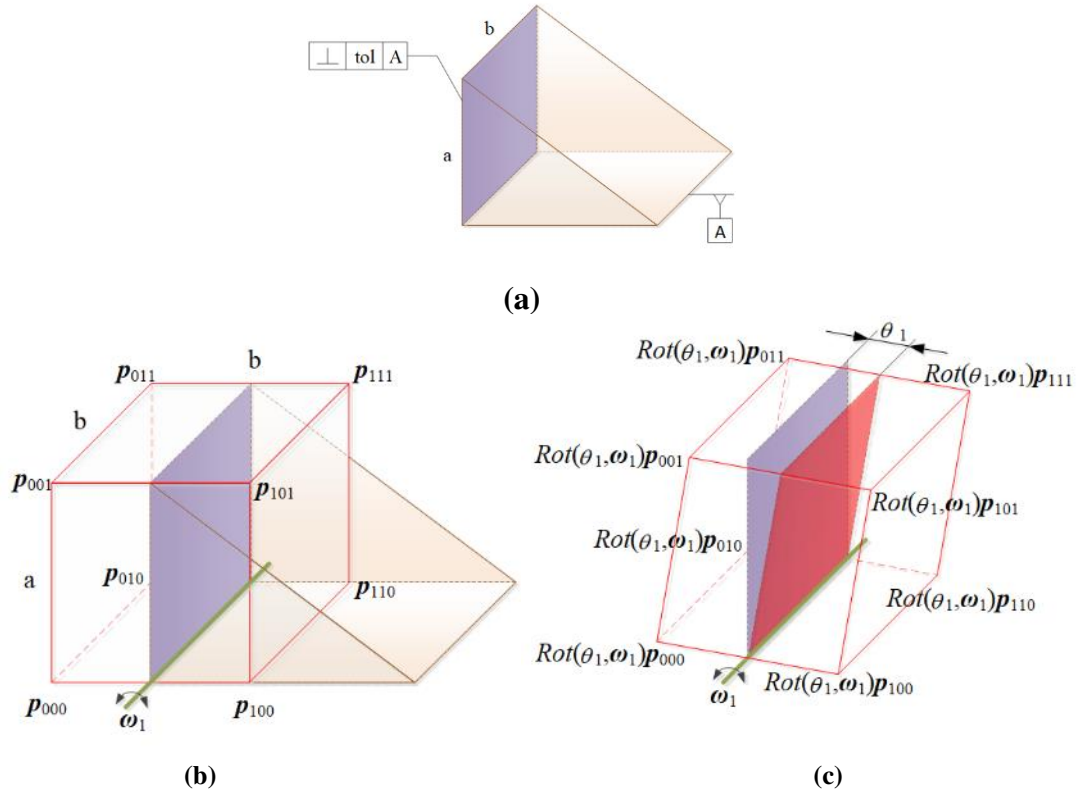
$$\mathbf{Q}'(s, u, w) = \sum_{i=0}^l \sum_{j=0}^m \sum_{k=0}^n B_i^l(s) B_j^m(u) B_k^n(w) \cdot \left( Rot(\theta_1, \boldsymbol{\omega}_1) Rot(\theta_2, \boldsymbol{\omega}_2) Rot(\theta_3, \boldsymbol{\omega}_3) \mathbf{p}_{ijk} \right) \quad (6)$$

where  $\boldsymbol{\omega}_1$ ,  $\boldsymbol{\omega}_2$  and  $\boldsymbol{\omega}_3$  are rotating axes (unit vector).  $\theta_1$ ,  $\theta_2$  and  $\theta_3$  are rotating angles about these

axes.  $Rot(\cdot, \cdot)$  is rotating matrix,  $Rot(\theta_i, \boldsymbol{\omega}_i) = \exp(\theta_i \hat{\boldsymbol{\omega}}_i)$  and  $\hat{\boldsymbol{\omega}}_i = \begin{bmatrix} 0 & -\omega_{i3} & \omega_{i2} \\ \omega_{i3} & 0 & -\omega_{i1} \\ -\omega_{i2} & \omega_{i1} & 0 \end{bmatrix}$  is an anti-

symmetric matrix [51], where  $\boldsymbol{\omega}_i = [\omega_{i1}, \omega_{i2}, \omega_{i3}]$ . As such, rotational tolerance zone can be modeled using Eq. (6).

In Fig. 3(a), a wedge shaped part has a perpendicular tolerance of  $tol$  in reference to datum plane A. Equivalently, this means the left plane can rotate about axis  $\omega$  by a maximal angle of  $\arctan(tol/a)$ . We can build a parametric space envelope as shown in Fig. 3(b). If all control points rotate about  $\omega_1$  axis by an angle of  $\theta_1$ , then the perpendicular tolerance zone can be calculated using Eq. (6) with permitted rotating angle to be in the range of  $-\arctan(tol/a) \leq \theta_1 \leq \arctan(tol/a)$  for the case in Fig. 3.



**Fig. 3** Perpendicular tolerance modeling based on parametric space envelope

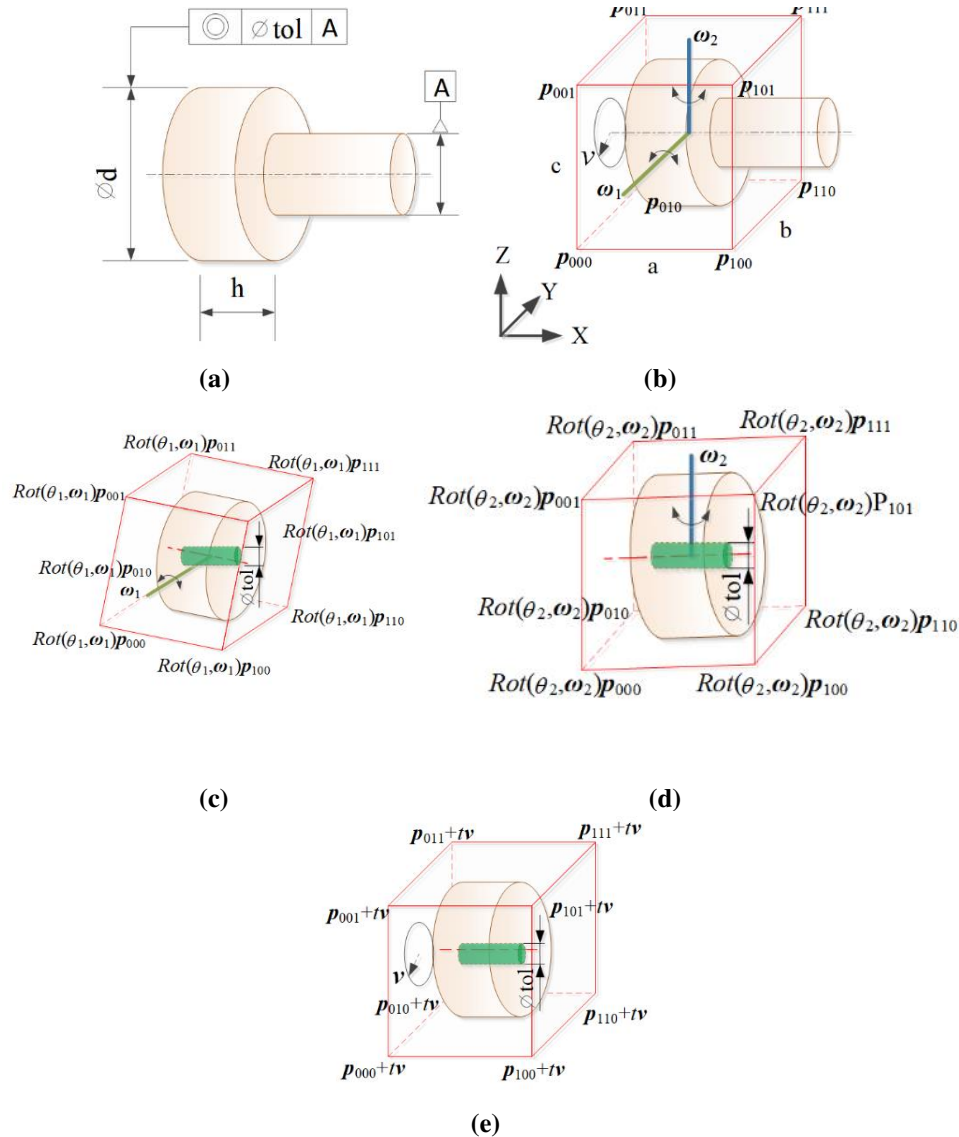
**3.2.3 Tolerance modeling for combined translational and rotational displacement.** If boundary control points are perturbed involving both translational and rotational movement, enclosed manufacturing part will experience both translational and rotational displacement. Concentricity is a tolerance (under GD&T standards) that controls the central axis of the referenced feature to a datum axis. The axes for the datum and referenced feature are derived from the median points of the part or feature. Concentricity is a three-dimensional cylindrical tolerance zone where all the derived median points of a referenced circular feature must fall into. Under proposed method, the displaced feature (under translational and rotational deviation of control points) is calculated as follows:

$$\mathbf{Q}'(s, u, w) = \sum_{i=0}^l \sum_{j=0}^m \sum_{k=0}^n B_i^l(s) B_j^m(u) B_k^n(w) (\text{Rot}(\theta_1, \omega_1) \text{Rot}(\theta_2, \omega_2) \text{Rot}(\theta_3, \omega_3) \mathbf{p}_{ijk} + t\mathbf{v}) \quad (7)$$

In Fig. 4(a), an intermediate shaft in transmission is composed of two different diameter sections which are coaxial. Datum A is the drive side and relatively fixed with bearings to the housing. The left referenced section is designed to be concentric with datum A to avoid oscillations at high speed. Specified concentricity tolerance  $tol$  is shown in Fig. 4(a). A parametric space envelope (or variation tool) is constructed and imposed on the target feature shown in Fig. 4(b). The displacement of the mating shaft from rotation about axis  $\omega_1$ , from rotation about axis  $\omega_2$  and from translation is shown in Fig. 4(c), Fig. 4(d) and Fig. 4(e), respectively. The tolerance zone is shown in Fig. 4(c). The location of displaced control points (after rotational and translational movement) is as follows:

$$\mathbf{p}'_{ijk} = \text{Rot}(\theta_1, \omega_1) \text{Rot}(\theta_2, \omega_2) \mathbf{p}_{ijk} + t\mathbf{v} \quad (8)$$

Combining Eqs. (7) and (8) with specified concentricity tolerance of  $tol$ , we can model the cylindrical tolerance zone as a function of rotational angle  $\theta_1$ , rotational angle  $\theta_2$  and translation distance  $t$ . If the mating shaft can only rotate about  $\omega_1$  with rotation about  $\omega_2$  and translational motion being restricted, permitted rotational angle range can be calculated as  $-\frac{tol}{h} \leq \theta_1 \leq \frac{tol}{h}$  in Fig. 4(c). Similarly, if only rotation about  $\omega_2$  is possible, permitted rotational angle  $\theta_2$  range is  $-\frac{tol}{h} \leq \theta_2 \leq \frac{tol}{h}$  in Fig. 4(d). If both rotations are restrained, allowed translational distance  $t$  in direction  $\mathbf{v}$  is  $-\frac{tol}{2} \leq t \leq \frac{tol}{2}$  in Fig. 4(e). If both rotation and translation deviation are possible,  $\theta_1$ ,  $\theta_2$  and  $t$  provide tradeoff between rotational and translational displacement based on Eqs. (7) and (8) subject to specified tolerance  $tol$ . In essence, rigid part related tolerance zone can be modeled by scaling and rotating the constructed parametric space envelope.



**Fig. 4** Concentricity tolerance modeling under parametric space envelope framework. (a) A mating shaft. (b) Constructed parametric space envelope. Left section of the shaft deviate from design intent from rotation about axis  $\omega_1$  (c), from rotation about axis  $\omega_2$  (d) and from translation displacement (e)

**3.3 Shape related tolerance modeling.** Under GD&T standards, form tolerance states how far an actual surface is permitted to vary from desired geometric form. Expressions of these tolerances refer to limits of flatness, straightness, circularity and cylindricity. Runout is how much a given reference feature varies with respect to another datum when the part is rotated  $360^\circ$  around the datum axis. Runout tolerance is used to control the location of a circular part feature relative to its axis. Profile tolerance of a surface describes a three-dimensional tolerance zone around a surface (similarly, profile tolerance of a line is a two-dimensional tolerance range that can be applied to any line in a feature). Profile tolerance controls all the points along the

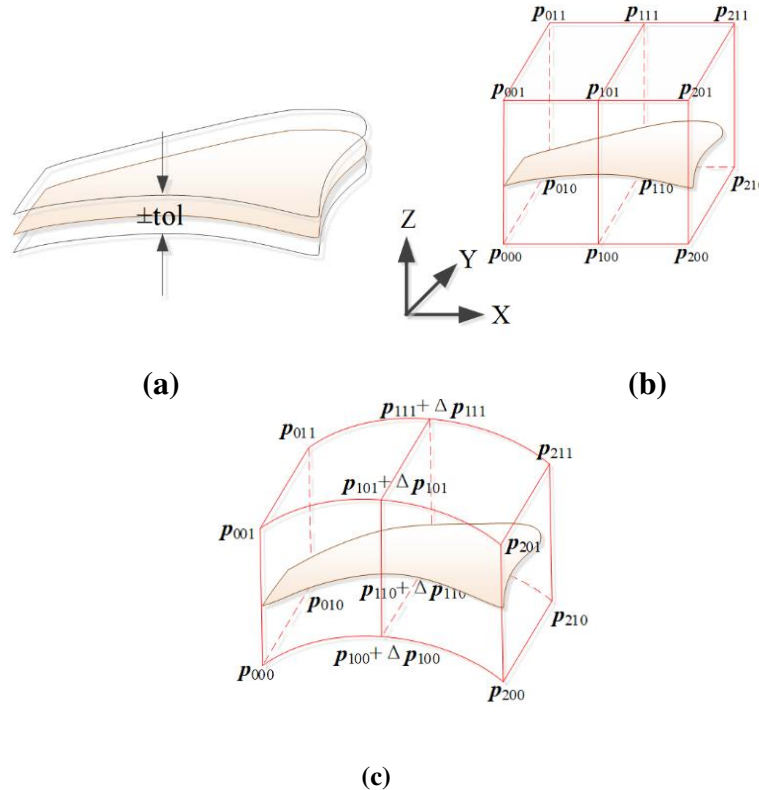


surface within a tolerance range that directly mimics the designed profile. Any point on the target surface would not be able to vary inside or outside by more than the surface profile tolerance.

Broadly speaking, these are all related to shape of a target feature (or part). Here we group them into shape-related tolerance which involves deformation modeling. More generally, geometric shape related tolerance is defined by two offset surfaces along the design intent under GD&T standards shown in Fig. 5. Deviation as well as deformation of a manufacturing part surface (plain or curved surface) can be modeled under proposed method. Deviation distance of the points on the deformed surface can be derived from Eq. (1):

$$d(s, u, w) = \sum_{i=0}^l \sum_{j=0}^m \sum_{k=0}^n B_i^l(s) B_j^m(u) B_k^n(w) (\mathbf{p}'_{ijk} - \mathbf{p}_{ijk}) \cdot \mathbf{n}(s, u, w) \quad (9)$$

where  $\mathbf{p}'_{ijk}$  and  $\mathbf{p}_{ijk}$  are the location of control points post deformation and pre deformation, respectively. And  $\mathbf{n}(s, u, w)$  is the normal at the point. Based on Eq. (9), the deviation of arbitrary points (randomly selected or sampled) can be obtained.  $d(s, u, w)$  is positive when projection of the deviation vector on to the normal is in accordance to the normal, otherwise  $d(s, u, w)$  is negative.



**Fig. 5** Profile tolerance modeling based on parametric space envelope

All actual features of the surface, falling within the tolerance zone, belong to an acceptable variational class. As such, allowable variation should be within the tolerance zone and satisfy the following constraint inequation:

$$|d(s, u, w)| \leq tol \quad (10)$$

With  $h$  sampled points on the target surface, Eq. (10) can be rewritten as

$$tol \geq |(\mathbf{a}_i \Delta \mathbf{P}) \cdot \mathbf{n}_i| \quad i = 1, 2, \dots, h \quad (11)$$

where  $\mathbf{a}_i = [B_0^l(s_i)B_0^m(u_i)B_0^n(w_i), \dots, B_i^l(s_i)B_m^m(u_i)B_n^n(w_i)]$  and  $\Delta \mathbf{p}^T = [\mathbf{p}'_{000} - \mathbf{p}_{000}, \dots, \mathbf{p}'_{N_p} - \mathbf{p}_{N_p}]$ . Because  $\mathbf{a}_i$  and  $\mathbf{n}_i$  are pre-computable, Eq. (11) can be further rewritten as

$$tol \geq |\mathbf{a}_i [\mathbf{n}_i, \dots, \mathbf{n}_i]^T \cdot \Delta \mathbf{p}| \quad i = 1, 2, \dots, h \quad (12)$$

The system of inequations in Eq. (12) builds the relationship between control points' movement and specified tolerance  $tol$ . Inequation (12) can be written in matrix:

$$\mathbf{T} \geq |\mathbf{A} \cdot \Delta \mathbf{p}| \quad (13)$$

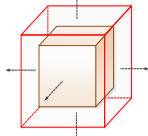
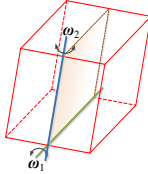
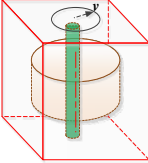
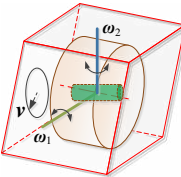
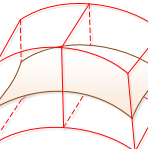
$$\text{Where } \mathbf{T} = [tol_1, \dots, tol_h]^T, \mathbf{A} = \begin{bmatrix} a_{11}n_{11} & a_{11}n_{12} & a_{11}n_{13} & , \dots, & a_{1N_p}n_{11} & a_{1N_p}n_{12} & a_{1N_p}n_{13} \\ & & & \mathbf{M} & & & \\ a_{h1}n_{h1} & a_{h1}n_{h2} & a_{h1}n_{h3} & , \dots, & a_{hN_p}n_{h1} & a_{hN_p}n_{h2} & a_{hN_p}n_{h3} \end{bmatrix}$$

and  $\Delta \mathbf{p}^T = [\Delta p_{000x} \quad \Delta p_{000y} \quad \Delta p_{000z} \quad ,L \quad \Delta p_{lmmx} \quad \Delta p_{lmmn} \quad \Delta p_{lmmx}]$  is the column vector of  $\Delta \mathbf{P}$ . Note that the proposed model can handle complex non-uniform tolerance, i.e. tolerance vector  $tol_l$  and  $tol_h$  can take different value. More details on non-uniform tolerance cases can be found in [50]. In essence, tolerance zone for complex free-form surface (or feature) is mapped into influence zone of control points under proposed modeling framework. As can be seen, with the tool of constructed parametric space envelope, full sets of GD&T tolerances can be modeled by the proposed methodology. Table 2 provides a summary on this.

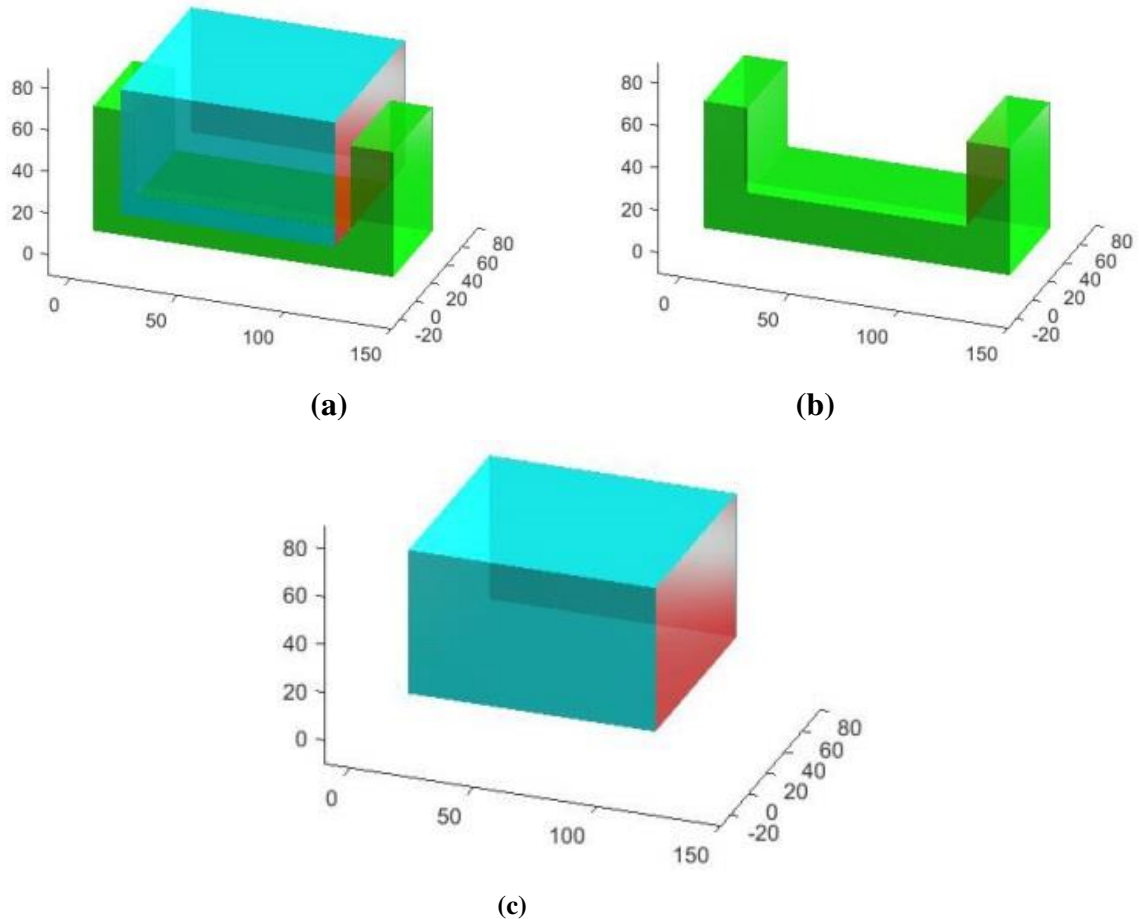
#### 4. Industrial case study

Tolerance analysis is routinely carried out by engineers to assess variation impact on products stemming from imperfections in manufactured parts. Below we apply developed method to tolerance analysis and synthesis (or allocation) on an industrial assembly.

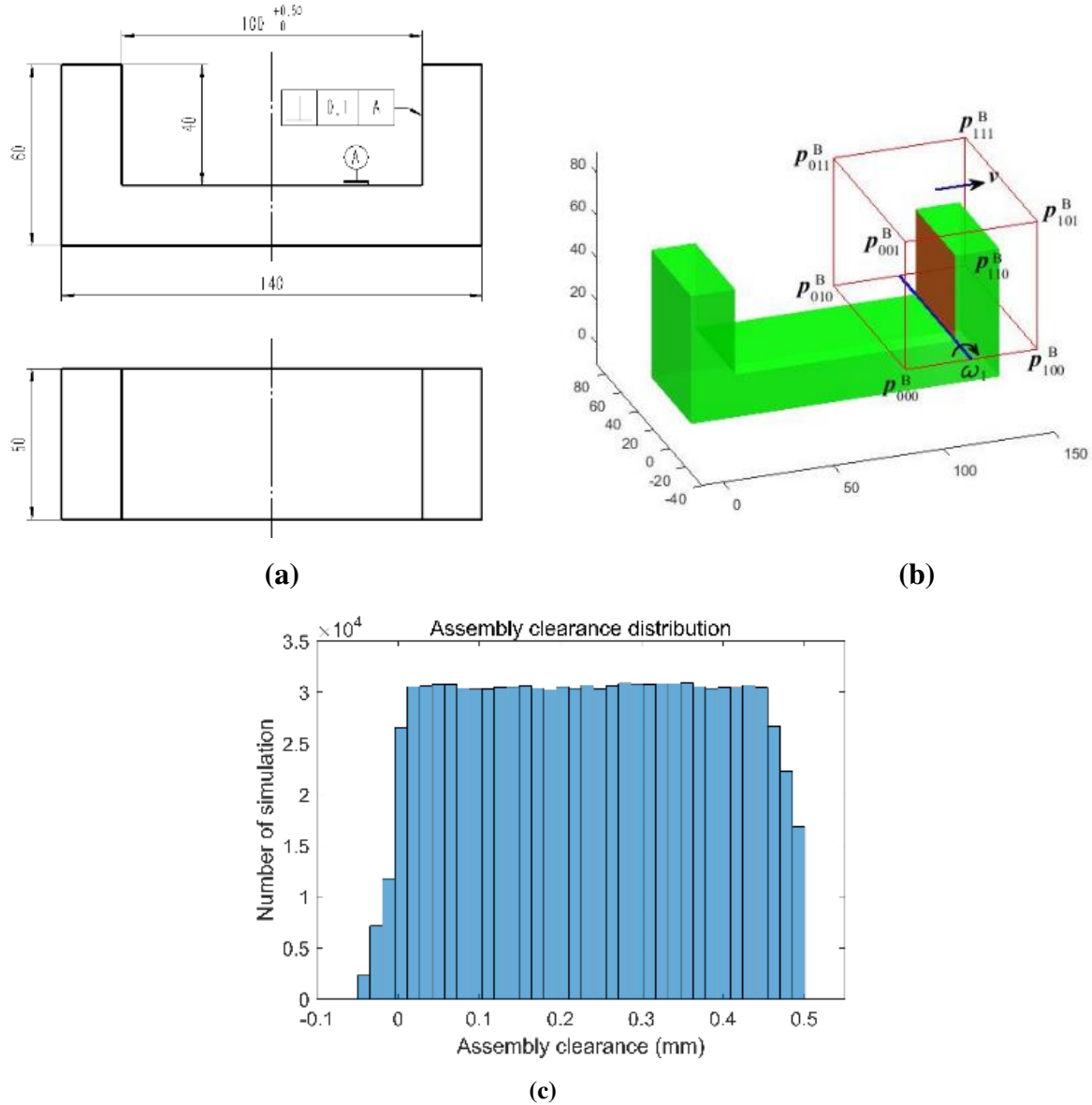
**Table 2 Dimensional and geometric tolerance modeling**

Types of tolerance		Characteristics	Control point movement	Illustration
Dimensional tolerance		Dimension	$\mathbf{p}_{ijk} + t_{ijk} \mathbf{v}_{ijk}$	
Rigid-body related tolerance	Orientation	Parallelism Perpendicularity Angularity	$Rot(\theta_1, \omega_1) Rot(\theta_2, \omega_2) \mathbf{p}_{ijk}$	
	Location	Position	$\mathbf{p}_{ijk} + t\mathbf{v}$	
	Combination	Concentricity Symmetry	$Rot(\theta_1, \omega_1) Rot(\theta_2, \omega_2) \mathbf{p}_{ijk} + t\mathbf{v}$	
Shape related tolerance	Form	Straightness Flatness Circularity Cylindricity	$\mathbf{p}_{ijk} + \Delta \mathbf{p}_{ijk}$	

In Fig. 6, a rectangular part is to be mated into the base part. The dimension of the referenced mating part is 100 mm × 90 mm × 60 mm. The length of the base part is 140 mm with height of 60 mm and width of 50 mm. Length of the slot in the base part is 100 mm with a tolerance of 0.5 mm shown in Fig. 7(a). And the slot in the base is also assigned with a perpendicular tolerance of 0.1 mm shown in Fig. 7(a).



**Fig. 6** Geometry of experiment parts in a two-part assembly (with unit in mm)



**Fig. 7** (a) Tolerance of the base part in Fig. 6, (b) constructed parametric space envelope is imposed on the target feature, and (c) assembly clearance distribution (only taking into account dimension and perpendicular tolerance)

To apply the developed method, a parametric space envelope with size of 60 mm  $\times$  90 mm  $\times$  60 mm has been constructed and imposed on the target feature in Fig. 7(b). The variation tool is positioned as such that target feature (the right plane of the slot) sits on the central line of the envelope's bottom. Eight control points  $p_{ijk}^B$  ( $i, j, k = 0, 1$ ) are located at the eight vertices of the rectangular block. If control points rotate around axis  $\omega_1$  by an angle of  $\theta_1$  and then

translationally displaced in direction  $\mathbf{v}$  by distance  $t_1$ , the position of displaced control points are as follows:

$$\mathbf{p}_{ijk}^{B'} = \text{Rot}(\theta_1, \boldsymbol{\omega}_1) \mathbf{p}_{ijk}^B + t_1 \mathbf{v} \quad (14)$$

When  $t_1$  is positive, i.e. control points moving in direction  $\mathbf{v}$ , the enclosed slot length increases. On the other hand, slot length gets shortened when control points move in opposite (or negative) direction with  $t_1 < 0$ .  $\theta_1$  and  $\boldsymbol{\omega}_1$  follows the right hand screw rule, i.e. the rotation in Fig. 7(b) is in the direction of positive rotation. The displaced feature (within the parametric space envelope) can be calculated as follows:

$$\mathbf{Q}'(s, u, w) = \sum_{i=0}^1 \sum_{j=0}^1 \sum_{k=0}^1 B_i^1(s) B_j^1(u) B_k^1(w) \cdot \left[ \text{Rot}(\theta_1, \boldsymbol{\omega}_1) \mathbf{p}_{ijk}^B + t_1 \mathbf{v} \right] \quad (15)$$

*A. Base part deviation.* If we only consider base part variation and assume the mating part is in nominal dimension, allowed control point translational displacement  $t_1$  is  $t_1 \in [0, 0.5]$  given the dimensional tolerance of  $[0, 0.5]$  in Fig. 7. Given the perpendicularity tolerance of 0.1 mm, permitted rotating angle  $\theta_1$  range (measured in radians) is  $\theta_1 \in \left[ -\frac{1}{800}, \frac{1}{800} \right]$  based on the constructed parametric space envelope in Fig. 7(b). Given the allowable range of  $t_1$  and  $\theta_1$ , permissible movement range of control points can be calculated from Eq. (14). If we simulate control points' random movements within their permitted range of  $t_1$  and  $\theta_1$ , we will get various deviated base part from Eq. (15). We then verify if the two-part assembly is successful or not based upon the criteria whether there is any interference between the two mating parts.

The `rand()` function in MATLAB is used to generate random numbers for  $t_1$  and  $\theta_1$  within their permitted range. Fig. 7(c) shows the experiment results based on 1,000,000 random simulatins. If the distance between the ideal mating part and the deviated base part is negative, i.e. there is interference, the assembly is not successful. In this simulation experiment, there is around 2.5% cases leading to failed assembly.

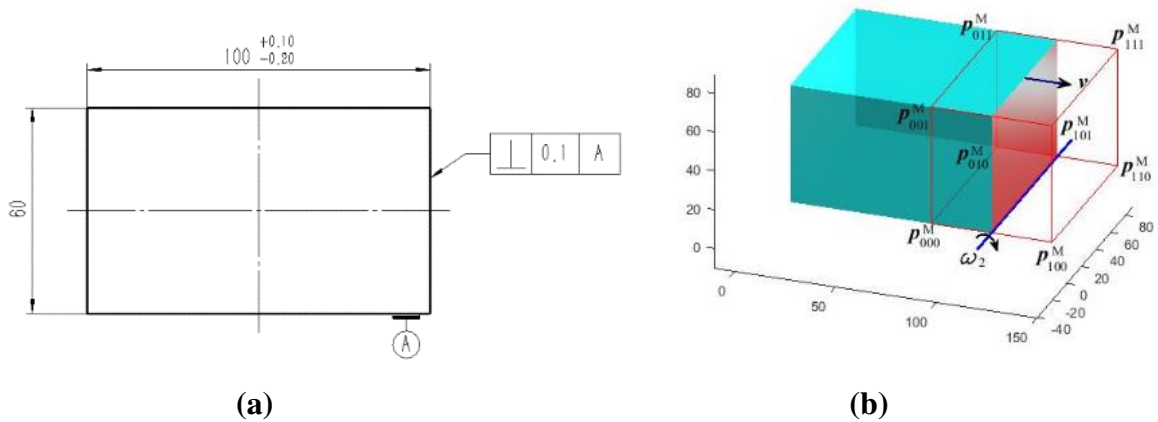
*B. Mating part deviation.* We now focus on deviation of the rectangular mating part and assume the base part is in nominal geometry. Dimensional tolerance (on the mating part length) is specified with an upper limit of 0.1 mm and lower limit of -0.2 mm in Fig. 8(a). Also there

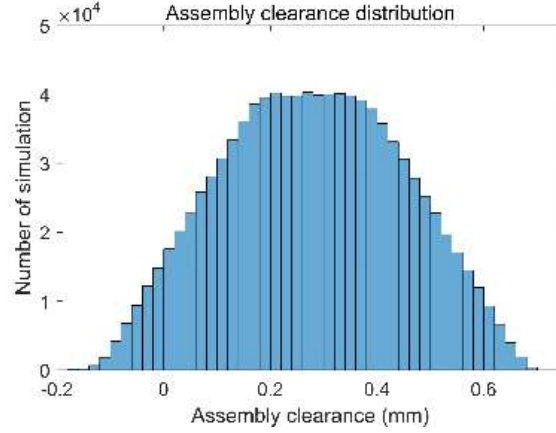
is a perpendicularity tolerance of 0.1 mm in reference to datum plane A. To apply the proposed method, a parametric space envelope is constructed and imposed on the target feature shown in Fig. 8(b). The size of the parametric space envelope is 60 mm × 90 mm × 60 mm. The parametric space envelope is positioned as such that the mating part's right plane sits on the central line of the bottom plane of the constructed variation tool. There are eight control points  $\mathbf{p}_{ijk}^M$  ( $i, j, k = 0, 1$ ) sitting at the vertices of the parametric space envelope.

The position of displaced control points, after rotation about axis  $\omega_2$  by an angle of  $\theta_2$  and translational movement of  $t_2$  in direction  $\mathbf{v}$ , is:

$$\mathbf{p}_{ijk}^{M'} = Rot(\theta_2, \omega_2) \mathbf{p}_{ijk}^M + t_2 \mathbf{v} \quad (16)$$

Given the dimensional tolerance of  $[-0.2, 0.1]$  in Fig. 8(a), permitted control points' translational distance  $t_2$  range is  $t_2 \in [-0.2, 0.1]$ . For assigned perpendicularity tolerance of 0.1 mm, allowed control point rotational angle  $\theta_2$  range is  $\theta_2 \in \left[-\frac{1}{1200}, \frac{1}{1200}\right]$  based on the constructed variation tool in Fig. 8(b). Simulating control points' random movement (within the allowed range of  $t_2$  and  $\theta_2$ ), we can analyze and assess the assembly of a deviated mating part and a nominal base part. Simulating 1,000,000 times of random control points' movements to get displaced mating part from Eq. (15), the distance between displaced mating part and nominal base part is shown in Fig. 8(c). It can be seen that around 5% of the simulated cases lead to failed assembly.





(c)

**Fig. 8** (a) Tolerance of the mating part in Fig. 6, (b) constructed parametric space envelope is imposed on the target feature, and (c) assembly clearance distribution

*C. Assembly tolerance allocation.* In above two experiments, 2.5% and 5% failure rates lead to unbearable scrap rate. And the tolerance needs to be adjusted to meet industry's  $3\sigma$  requirement, i.e. the parts need to be assembled successfully 99.73% ( $\pm 3\sigma$ ) of the time statistically. For illustration purpose, here we adjust mating part perpendicularity tolerance while keeping (both parts') dimensional tolerance and base part perpendicularity tolerance unchanged. In this case, the mating part and base part share same parametric space envelope (Fig. 7(b) and Fig. 8(b)). The distance of the two mating planes (red highlighted in Fig. 6) can be calculated as follows:

$$d(s, u, w) = \sum_{i=0}^1 \sum_{j=0}^1 \sum_{k=0}^1 B_i^1(s) B_j^1(u) B_k^1(w) \left[ (Rot(\theta_1, \omega_1) - Rot(\theta_2, \omega_2)) \mathbf{p}_{ijk} + (t_1 - t_2) \mathbf{v} \right] \cdot \mathbf{v} \quad (17)$$

Note distance  $d$  can be positive or negative number. Given  $\mathbf{v}$  is normal to the mating plane, Eq. (17) can be written as

$$d(s, u, w) = \sum_{i=0}^1 \sum_{j=0}^1 \sum_{k=0}^1 B_i^1(s) B_j^1(u) B_k^1(w) \left[ \left[ (Rot(\theta_1, \omega_1) - Rot(\theta_2, \omega_2)) \mathbf{p}_{ijk} \right]^T \cdot \mathbf{v} + (t_1 - t_2) \right] \quad (18)$$

For the two-part assembly to be successful, the distance  $d$  has to be non-negative, i.e.  $d \geq 0$ . Since  $\omega_1$  and  $\omega_2$  is essentially rotating around the same axis, Eq. (18) can be further written as:

$$d(s, u, w) \approx \sum_{i=0}^1 \sum_{j=0}^1 \sum_{k=0}^1 B_i^1(s) B_j^1(u) B_k^1(w) \left[ \left[ (\theta_1 - \theta_2) \hat{\omega} \mathbf{p}_{ijk} \right]^T \cdot \mathbf{v} + (t_1 - t_2) \right] \quad (19)$$



where  $\hat{\omega}$  is the anti-symmetric matrix of  $\omega$ . Here assembly distance  $d$  is a function of  $t_1$ ,  $t_2$ ,  $\theta_1$  and  $\theta_2$ . With slot length tolerance of  $[0, 0.5]$  in Fig. 7(a) and dimensional tolerance for the mating part of  $[-0.3, 0]$ ,  $t_1$  and  $t_2$  allowed range is  $t_1 \in [0, 0.5]$  and  $t_2 \in [-0.3, 0]$ . Permitted rotating range for angle  $\theta_1$  is  $[-\frac{1}{800}, \frac{1}{800}]$  based on base part perpendicularity tolerance of 0.1 mm in Fig. 7(a) and the constructed variation tool. Set perpendicularity tolerance of the mating part to be  $a$ , then permitted rotating angle range for  $\theta_2$  is  $[-\frac{a}{120}, \frac{a}{120}]$ . Simulating control points' movement based upon permitted range for  $t_1$ ,  $t_2$ ,  $\theta_1$  and  $\theta_2$ , the assembly distance can be calculated from Eq. (19). Table 3 provides the results based on 1,000,000 simulations.

It can be seen from Table 3 that the assembly will meet  $\pm 3\sigma$  requirement when variable  $a$  takes the value of 0.14. In this case, the perpendicularity tolerance is 0.14 mm. The corresponding permitted rotation angle  $\theta_2$  range to be  $[-\frac{7}{6000}, \frac{7}{6000}]$ , and the assembly yield is 99.7409%.

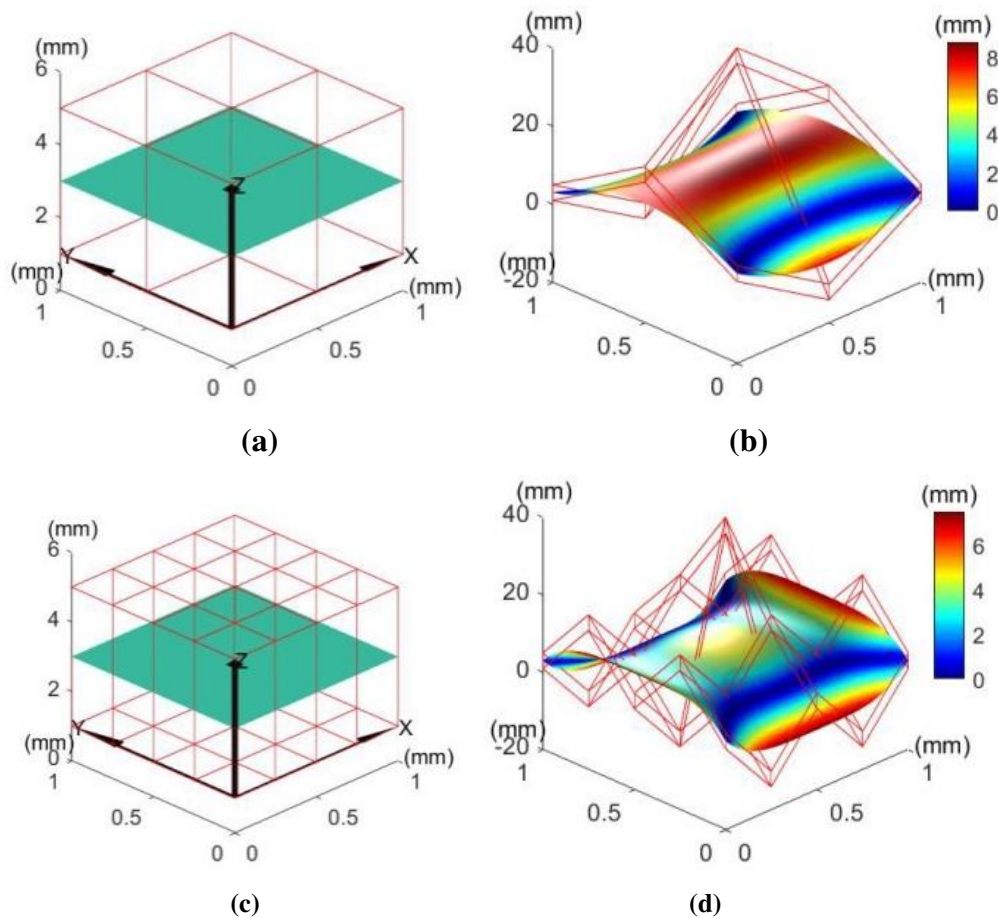
**Table 3 Parameter  $a$  and the corresponding assembly rate**

$a$	Compliance assembly rate $P$
0.05	99.8407%
0.10	99.7981%
0.11	99.7902%
0.12	99.7624%
0.13	99.7565%
0.14	99.7409%
0.15	99.7230%
0.20	99.6160%

## 5. Model discussion

Using parametric space envelope, this paper developed a unified geometric variation model that bridges manufacturing and design. The proposed methodology is versatile and can cover whole sets of tolerances specified by GD&T standards. It helps formalize GD&T tolerance specification. Due to its unique modeling through constructed variation tool, it can model rigid part deviation as well as geometric deformation experienced by non-rigid compliant part. For ease of illustration, the aforementioned parametric space envelope is constructed from

a Bezier curve. The resulting variation tool is a trivariate Bezier volume. In real application, other parametric curves (i.e., B-splines, NURBS among others) can be selected to construct the variation tool. To facilitate illustration, the aforementioned variation tool is constructed with just eight control points. In practical application, user can construct the variation tool with more control points to get diverse geometric variation to mimic real variations observed in production. Figure 9 shows the impact with more control points being added. However, it is worth noting that computation costs will go up when more control points being selected to construct the variation tool.



**Fig. 9** Deformation impact by adding more control points. (a-b) Deformation of a plain sheet metal under variation tool with 18 control points. (c-d) Deformation of the same plain sheet metal under variation tool with 50 control points

The difficulty in tolerance related geometric variation modeling lies in correctly capturing intra-part interactions. These interactions induced by geometric variation are non-linear in general. Approximation on this can drag down modeling accuracy considerably. Through

constructing a variation tool, the proposed method circumvents direct modeling these interactions. Instead, the modeling is conducted through envelope’s boundary control points. This indirect modeling brings various benefits including modeling accuracy for handling complex manufacturing part. In addition, proposed method has added advantage of modeling efficiency. There are typically multiple tolerances specified on the same manufacturing part, i.e. dimensional, flatness and perpendicular tolerance. With existing methods, user typically needs to model them separately, and then do the stack-up analysis and calculation in extra steps. Under proposed methodology, these tolerances can be modeled and handled more efficiently with stack-up analysis being done centrally around control points’ movement.

Nowadays various computer-aided systems are extensively used in industry to improve product design and manufacturing. Note the modeling framework developed in this paper is based upon parametric space envelope which is a variation tool constructed from base parametric curves. These parametric curves are widely used in the CAD system [52, 53]. As such, our CAD-driven approach will facilitate integration of existing CAD and PLM systems with tolerancing to meet industry’s emerging demands in a new era of digital manufacturing.

## **6. Conclusion and Future Work**

This paper has developed a framework and methodology for tolerance modeling under GD&T standards. This framework is based on parametric space envelope, a variation tool constructed to aid tolerance modeling. Under proposal, complex geometric tolerance is modeled through a compact set of control points, and related tolerance zone is converted to control point influence zone. The proposed method is comprehensive in that it can model all classes of tolerance specified in the standards. It is versatile that it can handle both rigid and non-rigid compliant parts, simple as well as complex manufacturing parts. It aims to give manufacturing firm a competitive edge in a new era of digital manufacturing.

Our proposal shows great application potential. Equipped with developed methodology, user can assess part variation impact by generating various geometric errors of target part through simulating boundary control points’ movement; User could also link “geometric errors pattern of target part” to tolerances of part’s functional requirements (key product

*Cite as:* Chen, L., Franciosa, P., Zhijie, M., Ceglarek, D., 2020, “A Unified Framework for Tolerance Modeling and Analysis Based on Parametric Space Envelope”, *ASME Trans., Journal of Manufacturing Science and Engineering*, Vol. 142, No. 6, Article No. 061007, June 2020, DOI: <https://doi.org/10.1115/1.4046743>.

characteristics<sup>1</sup>, KPCs [54]) taking into account process requirements (key control characteristics<sup>2</sup>, KCCs). User could further link KCCs variation pattern to KCCs tolerance. Our future work includes exploring these application potentials in variation analysis [55, 56], manufacturing quality control [57, 58], tolerance analysis [59] and tolerance synthesis [60].

## **Acknowledgment**

This work was carried out in collaboration with the Digital Lifecycle Management research group from University of Warwick in the UK. This study is also partially supported by China Scholarship Council (on behalf of the Chinese Ministry of Education) and the National Natural Science Foundation of China under grant No. 51975119 and No. 51575107. The support is gratefully acknowledged.

---

<sup>1</sup> An example of KPC is dimension of the target part.

<sup>2</sup> For example, fixture locators' position errors are the dimensional control characteristics for product positioning, and thus are the determining factors in achieving the required dimensional accuracy. These are referred to as Key Control Characters.

## Nomenclature

- $B_i^l(s)$  = Bernstein polynomial of degree  $l$
- $s$  = parameter of Bernstein polynomials,  $0 \leq s \leq 1$
- $u$  = parameter of Bernstein polynomials,  $0 \leq u \leq 1$
- $w$  = parameter of Bernstein polynomials,  $0 \leq w \leq 1$
- $l$  = degree of Bernstein polynomials
- $m$  = degree of Bernstein polynomials
- $n$  = degree of Bernstein polynomials
- $P_{ijk}$  = the  $i, j, k$ -th control point
- $\mathbf{Q}$  = sample point on target feature
- $\Delta\mathbf{Q}$  = deviation of sample point  $\mathbf{Q}$  on target feature
- $t$  = control point translational moving distance
- $\mathbf{v}$  = control point translational motion direction
- $tol$  = specified tolerance under GD&T standards
- $\boldsymbol{\omega}$  = rotating axis
- $\theta$  = rotating angle
- $Rot(\cdot, \cdot)$  = rotating matrix
- $d(s, u, w)$  = deviation distance of a point  $X(s, u, w)$  on target part
- $\mathbf{n}(s, u, w)$  = the normal at the point  $X(s, u, w)$
- $\mathbf{A}$  = geometric mapping matrix
- $r_j$  = radius of  $j$ -th control point movement in its local sphere
- $\mathbf{T}$  = vector of tolerance  $\mathbf{T} = [tol_1, L, tol_h]^T$
- $P$  = assembly rate
- CAD** = computer-aided design
- FFD** = free-form deformation
- PLM** = product lifecycle management
- DOF** = degree of freedom

## References

- [1] DeFeo, J. A., and Juran, J. M., 2016, “The complete guide to performance excellence,” *Juran's quality handbook*, McGraw-Hill Education.
- [2] Aderiani, A. R., Wärmefjord, K., and Söderberg, R., 2018, “A Multistage Approach to the Selective Assembly of Components without Dimensional Distribution Assumptions,” *Journal of Manufacturing Science and Engineering.*, **140**(7), p. 071015.
- [3] Sadeghi T. R., Wärmefjord, K., Söderberg, R., and Lindkvist, L., 2019, “A Novel Rule-Based Method for Individualized Spot Welding Sequence Optimization With Respect to Geometrical Quality.” *ASME. J. Manuf. Sci. Eng.*, **141**(11), p. 111013.
- [4] Singh, A., and Agrawal, A., 2018, “Investigation of Parametric Effects on Geometrical Inaccuracies in Deformation Machining Process.” *ASME. J. Manuf. Sci. Eng.*, **140**(7), p. 074501.
- [5] Bastani, K., Barazandeh, B., and Kong, Z., 2018, “Fault Diagnosis in Multistation Assembly Systems Using Spatially Correlated Bayesian Learning Algorithm.” *ASME. J. Manuf. Sci. Eng.*, **140**(3), p. 031003.
- [6] Tahan, A., and Cauvier, J., 2012, “Capability Estimation of Geometrical Tolerance With a Material Modifier by a Hasofer–Lind Index,” *ASME. J. Manuf. Sci. Eng.*, **134.**, p. 021007.
- [7] Requicha, A. A., and Stephen C. C., 1985, “Representation of geometric features, tolerances and attributes in solid modellers based on constructive solid geometry,” *Production Automation Project*, University of Rochester.
- [8] Meadows, J. D., 2017, “Geometric Dimensioning and Tolerancing: Applications and Techniques for Use in Design: Manufacturing, and Inspection,” *Routledge*.
- [9] American Society of Mechanical Engineers. ASME., 2013, Y14.5-2009—dimensioning and tolerancing. New York.
- [10] ISO, 2017, Geometrical Product Specifications (GPS)—geometrical tolerancing—Tolerances of form, orientation, location and run-out, ISO Standard.
- [11] Ngoi, B. K. A., 1992, “Applying linear programming to tolerance chart balancing,” *The International Journal of Advanced Manufacturing Technology*, **7** (4), pp.187-192.
- [12] Shen, Z., Shah, J. J., and Davidson, J. K., 2003, “Automation of Linear Tolerance Charts and Extension to Statistical Tolerance Analysis,” *Journal of Computing and Information Science in Engineering*, **3**(1), pp. 95–99.
- [13] Sacks, E., and Joskowicz, L., 1998, “Parametric kinematic tolerance analysis of general planar systems,” *Computer-Aided Design.*, **30**(9), pp.707–714.
- [14] Desrochers, A., and Clément, A., 1994, “A dimensioning and tolerancing assistance model for CAD/CAM systems,” *The International Journal of Advanced Manufacturing Technology.*, **9**(6), pp. 352–361.
- [15] Giordano, M., Samper, S., and Petit, J. P., 2007, “Tolerance analysis and synthesis by means of deviation domains, axi-symmetric cases,” *Models for computer aided tolerancing in design and manufacturing*, pp. 85-94.
- [16] Davidson, J. K., Mujezinovic, A., and Shah, J. J., 2002, “A new mathematical model for geometric tolerances as applied to round faces,” *Journal of mechanical design*, **124**(4), pp. 609-622.
- [17] Desrochers, A., Ghie, W., and Laperriere, L., 2003, “Application of a unified Jacobian–Torsor model for tolerance analysis,” *ASME J Comput Inf Sci Eng.*, **3**(1), pp. 2–14.

*Cite as:* Chen, L., Franciosa, P., Zhijie, M., Ceglarek, D., 2020, “A Unified Framework for Tolerance Modeling and Analysis Based on Parametric Space Envelope”, *ASME Trans., Journal of Manufacturing Science and Engineering*, Vol. 142, No. 6, Article No. 061007, June 2020, DOI: <https://doi.org/10.1115/1.4046743>.

- [18] Liu, Y. and Xu, X., 2017, “Industry 4.0 and cloud manufacturing: A comparative analysis,” *ASME J. Manuf. Sci. Eng.*, **139**(3), p.034701.
- [19] Chong, L., Ramakrishna, S., and Singh, S., 2018, “A review of digital manufacturing-based hybrid additive manufacturing processes,” *The International Journal of Advanced Manufacturing Technology*, **95**(5-8), pp. 2281-2300.
- [20] Sarvari, P. A., Ustundag, A., Cevikcan, E., Kaya, I., and Cebi, S., 2018, “Technology roadmap for Industry 4.0,” *Industry 4.0: Managing The Digital Transformation*, Springer, Cham, pp. 95-103.
- [21] Boschert, S., and Rosen, R., 2016, “Digital twin—the simulation aspect,” *Mechatronic Futures*, Springer, Cham, pp. 59-74.
- [22] Franciosa, P., Gerbino, S., Lanzotti, A., and Patalano, S., 2013, “Automatic evaluation of variational parameters for tolerance analysis of rigid parts based on graphs,” *International Journal on Interactive Design and Manufacturing (IJIDeM)*, **7**(4), pp. 239-248.
- [23] Requicha, A. A., 1983, “Toward a theory of geometric tolerancing.” *The International Journal of Robotics Research*, **2**(4), pp. 45-60.
- [24] Adragna, P. A., Samper, S., and Pillet, M., 2009, “A proposition of 3D inertial tolerancing to consider the statistical combination of the location and orientation deviations,” *International Journal of Product Development*, **10** (1-3), pp. 26-45.
- [25] Clément, A., 1991, “Theory and practice of 3-D tolerancing for assembly,” *Proc. CIRP Int. Working Seminar on Computer-Aided Tolerancing.*, vol. 25.
- [26] Laperriere, L., Ghie, W., and Desrochers, A., 2002, “Statistical and deterministic tolerance analysis and synthesis using a unified Jacobian–Torsor model,” *CIRP Ann— Manuf Technol.*, **51**(1), pp. 417–20.
- [27] Ghie, W., 2009, “Statistical analysis tolerance using Jacobian Torsor model based on uncertainty propagation method”, *Int J Multiphys.*, **3**(1), pp. 11–30.
- [28] Ghie, W., Laperriere, L., and Desrochers, A., 2010, “Statistical tolerance analysis using the unified Jacobian–Torsor model”, *Int J Prod Res.*, **48**(15), pp. 4609–30.
- [29] Chen, H., Jin, S., Li, Z., and Lai, X., 2015, “A modified method of the unified Jacobian-Torsor model for tolerance analysis and allocation,” *International Journal of Precision Engineering and Manufacturing*, **16**(8), pp. 1789-1800.
- [30] Zeng, W., Rao, Y., Wang, P., and Yi, W., 2017, “A solution of worst-case tolerance analysis for partial parallel chains based on the Unified Jacobian-Torsor model,” *Precision Engineering*, **47**, pp. 276-291.
- [31] Jin, S., Ding, S., Li, Z., Yang, F., and Ma, X., 2018, “Point-based solution using Jacobian-Torsor theory into partial parallel chains for revolving components assembly,” *Journal of manufacturing systems*, **46**, pp. 46-58.
- [32] Ameta, G., Serge, S., and Giordano, M., 2011, “Comparison of spatial math models for tolerance analysis: tolerance-maps, deviation domain, and TTRS,” *Journal of Computing and Information Science in Engineering*, **11**(2), p.021004.
- [33] Ameta, G., Singh, G., Davidson, J. K., and Shah, J. J., 2018, “Tolerance-Maps to Model Composite Positional Tolerancing for Patterns of Features,” *Journal of Computing and Information Science in Engineering*, **18**(3), p. 031003.
- [34] Tiwary, H. R., 2007, “On the hardness of minkowski addition and related operations,” *Proceedings of the twenty-third annual symposium on Computational geometry*, pp. 306-309.

*Cite as:* Chen, L., Franciosa, P., Zhijie, M., Ceglarek, D., 2020, "A Unified Framework for Tolerance Modeling and Analysis Based on Parametric Space Envelope", *ASME Trans., Journal of Manufacturing Science and Engineering*, Vol. 142, No. 6, Article No. 061007, June 2020, DOI: <https://doi.org/10.1115/1.4046743>.

- [35] Desrochers, A., and Clément, A., 1994, "A dimensioning and tolerancing assistance model for CAD/CAM systems," *The International Journal of Advanced Manufacturing Technology*, **9**(6), pp. 352-361.
- [36] Clément, A., Riviere, A., Serré, P., and Valade, C., 1998, "The TTRSs: 13 Constraints for Dimensioning and Tolerancing Geometric Design Tolerancing: Theories, Standards and Applications," ElMaraghy, H.A. (Ed.): Chapman and Hall, London, pp.122-131.
- [37] Liu, J., and Wilhelm, R. G., 2003, "Genetic algorithms for TTRS tolerance analysis," *Geometric Product Specification and Verification: Integration of Functionality*, pp. 73-82.
- [38] Desrochers, A., 2003, "A CAD/CAM representation model applied to tolerance transfer methods," *Journal of Mechanical Design*, **125**(1), pp. 14-22.
- [39] Cao, Y., Zhao, Q., Liu, T., Ren, L., and Yang, J., 2018, "The Strategy of Datum Reference Frame Selection Based on Statistical Learning," *Journal of Computing and Information Science in Engineering*, **18**(2), p. 021002.
- [40] Hong, Y. S., and Chang, T. C., 2002, "A comprehensive review of tolerancing research," *International Journal of Production Research*, **40**(11), pp. 2425-2459.
- [41] Chen, H., Jin, S., Li, Z., and Lai, X., 2014, "A comprehensive study of three dimensional tolerance analysis methods," *Computer-Aided Design*, **53**, pp.1-13.
- [42] Cao, Y., Liu, T., & Yang, J., 2018, "A comprehensive review of tolerance analysis models," *The International Journal of Advanced Manufacturing Technology*, **97**(5-8), pp. 3055-3085.
- [43] Cao Y., Liu T., Yang J. A., 2018, "A comprehensive review of tolerance analysis models." *The International Journal of Advanced Manufacturing Technology*, **97**(5-8), pp.1-31.
- [44] Marziale, M., and Polini, W., 2011, "A review of two models for tolerance analysis of an assembly: Jacobian and torsor," *International Journal of Computer Integrated Manufacturing*, **24**(1), 74-86.
- [45] Mansuy, M., Giordano, M., and Davidson, J. K., 2013, "Comparison of two similar mathematical models for tolerance analysis: T-Map and deviation domain," *Journal of Mechanical Design*, **135**(10), 101008.
- [46] Schleich, B., Anwer, N., Mathieu, L., and Wartzack, S., 2017, "Shaping the digital twin for design and production engineering," *CIRP Annals*, **66**(1), pp. 141-144.
- [47] Söderberg, R., Wärmefjord, K., Carlson, J. S., and Lindkvist, L., 2017, "Toward a Digital Twin for real-time geometry assurance in individualized production," *CIRP Annals*, **66**(1), pp. 137-140.
- [48] Tao, F., Cheng, J., Qi, Q., Zhang, M., Zhang, H., and Sui, F., 2018, "Digital twin-driven product design, manufacturing and service with big data," *The International Journal of Advanced Manufacturing Technology*, **94**(9-12), pp. 3563-3576.
- [49] Sederberg, T. W., and Parry, S. R., 1986, "Free-form deformation of solid geometric models," *ACM SIGGRAPH computer graphics*, **20**(4), pp. 151-160.
- [50] Luo, C., Franciosa, P., Ceglarek, D., Ni, Z., and Jia, F., 2018, "A Novel Geometric Tolerance Modeling Inspired by Parametric Space Envelope," *IEEE Transactions on Automation Science and Engineering*, **15**(3), pp. 1386-1398.
- [51] Murray, R. M., 2017, "A mathematical introduction to robotic manipulation," CRC press, ISBN-13: 9781138440166.
- [52] Farin, G. E., and Farin, G., 2002, "Curves and surfaces for CAGD: a practical guide," Morgan Kaufmann.



*Cite as:* Chen, L., Franciosa, P., Zhijie, M., Ceglarek, D., 2020, "A Unified Framework for Tolerance Modeling and Analysis Based on Parametric Space Envelope", *ASME Trans., Journal of Manufacturing Science and Engineering*, Vol. 142, No. 6, Article No. 061007, June 2020, DOI: <https://doi.org/10.1115/1.4046743>.

- [53] Sarcar, M. M. M., Rao, K. M., and Narayan, K. L., 2008, "Computer aided design and manufacturing," PHI Learning Pvt. Ltd..
- [54] Shiu, B. W., Apley, D. W., Ceglarek, D., & Shi, J. (2003), "Tolerance allocation for compliant beam structure assemblies," *IIE transactions.*, **35**(4), pp. 329-342.
- [55] Loose, J. P., Zhou, Q., Zhou, S., & Ceglarek, D. (2010)., "Integrating GD&T into dimensional variation models for multistage machining processes," *International Journal of Production Research*, **48**(11), pp. 3129-3149.
- [56] Yu, H., Zhao, C., and Lai, X., 2018, "Compliant Assembly Variation Analysis of Scalloped Segment Plates With a New Irregular Quadrilateral Plate Element Via ANCF." *ASME. J. Manuf. Sci. Eng.*, **140**(9), p. 091006.
- [57] Huang, W., Liu, J., Chalivendra, V., Ceglarek, D., Kong, Z., and Zhou, Y., 2014, "Statistical modal analysis for variation characterization and application in manufacturing quality control," *IIE Transactions.*, **46**(5), pp. 497-511.
- [58] Djurdjanovic D, Mears, L., Niaki, F., Haq, A., Li, L., 2018, "State of the Art Review on Process, System, and Operations Control in Modern Manufacturing," *ASME. J. Manuf. Sci. Eng.*, **140**(6), pp. 061010-061010-18.
- [59] Huang, W., Ceglarek, D., & Zhou, Z., 2004, "Tolerance analysis for design of multistage manufacturing processes using number-theoretical net method (NT-net)," *International Journal of Flexible Manufacturing Systems*, **16**(1), pp. 65-90.
- [60] Huang, W., Phoomboplab, T., & Ceglarek, D. (2009). "Process capability surrogate model-based tolerance synthesis for multi-station manufacturing systems," *IIE Transactions.*, **41**(4), pp. 309-322.